

## Electronic Supplementary Information

### Bimetallic Ni-Fe Phosphide Nanocomposites with Controlled Architecture and Composition Enabling Highly Efficient Electrochemical Water Oxidation

*Ping Li and Hua Chun Zeng\**

Department of Chemical and Biomolecular Engineering  
Faculty of Engineering, National University of Singapore  
119260, Singapore

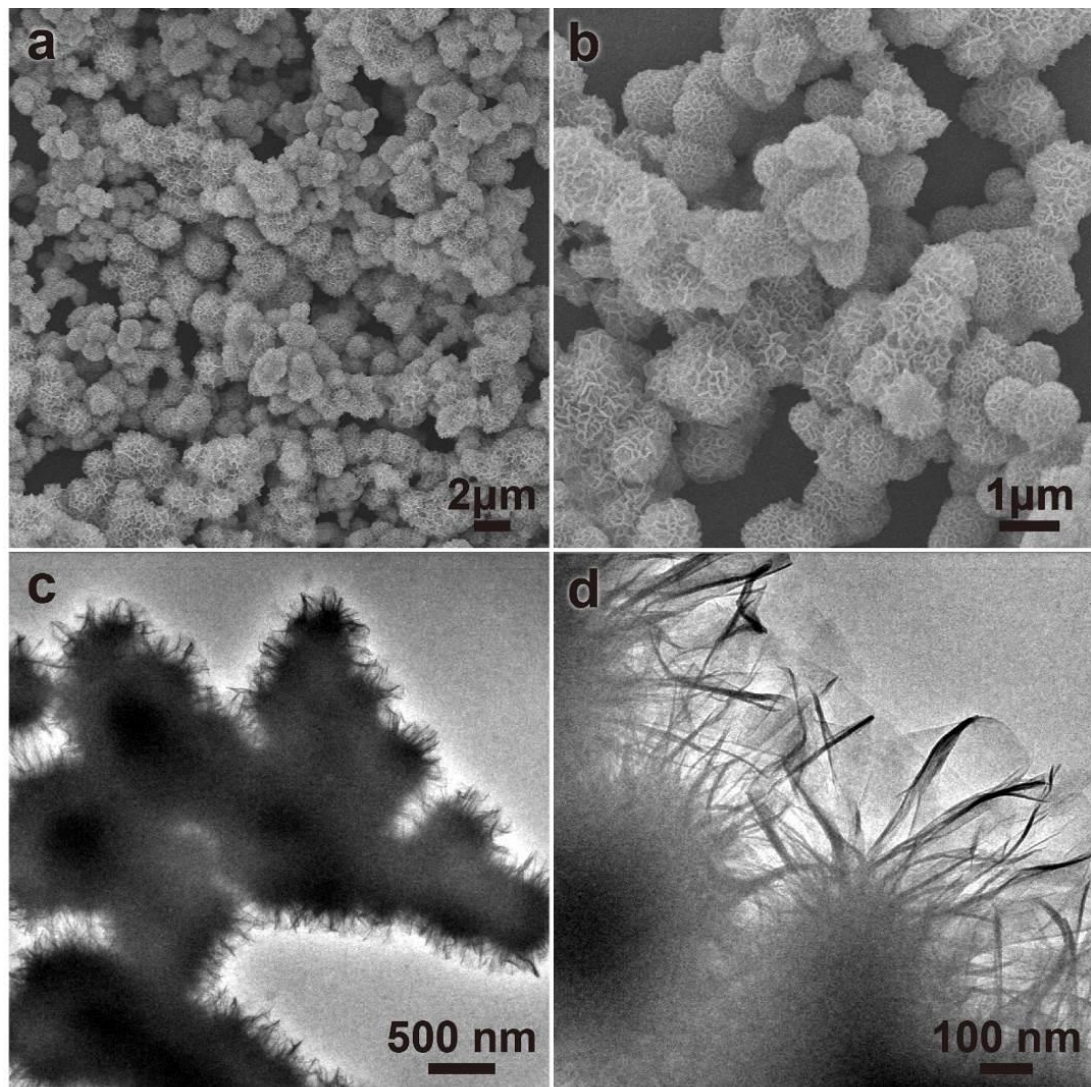
#### Table of Contents

Table S1 .....	Page 2
Figures S1 to S21 .....	Pages 3-23
Table S2 .....	Page 24
Figure S22 .....	Page 25
Table S3 .....	Page 26
References .....	Pages 27-28

**Additional experimental details for the preparation of NiFe(*n*:1)-LDH precursors:**

**Table S1.** The amount of metal salts used in the preparation of NiFe(*n*:1)-LDH precursors:

NiFe( <i>n</i> :1)-LDH	<i>n</i> (metal salt)/mmol	
	Ni(NO <sub>3</sub> ) <sub>2</sub> ·6H <sub>2</sub> O	Fe(NO <sub>3</sub> ) <sub>3</sub> ·9H <sub>2</sub> O
NiFe(1:1)-LDH	2 mmol	2 mmol
NiFe(3:1)-LDH	3 mmol	1 mmol
NiFe(5:1)-LDH	3.33 mmol	0.67 mmol
NiFe(7:1)-LDH	3.5 mmol	0.5 mmol
NiFe(9:1)-LDH	3.6 mmol	0.4 mmol



**Figure S1.** (a, b) SEM and (c, d) TEM images of the flowerlike NiFe(3:1)-LDH.

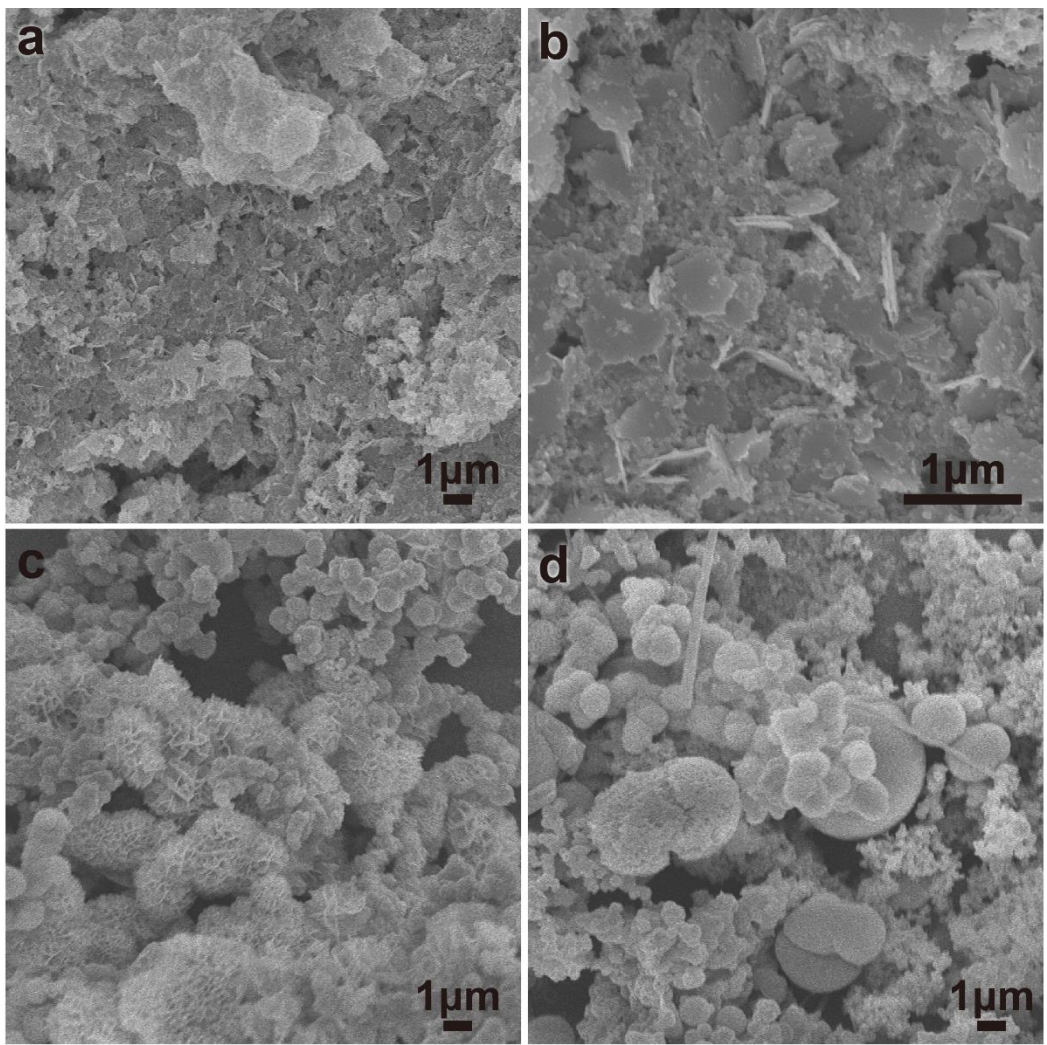


**Figure S2.** SEM images of the precursors prepared by using various solvents: (a, b) deionized water, (c) ethanol, and (d) isopropanol.

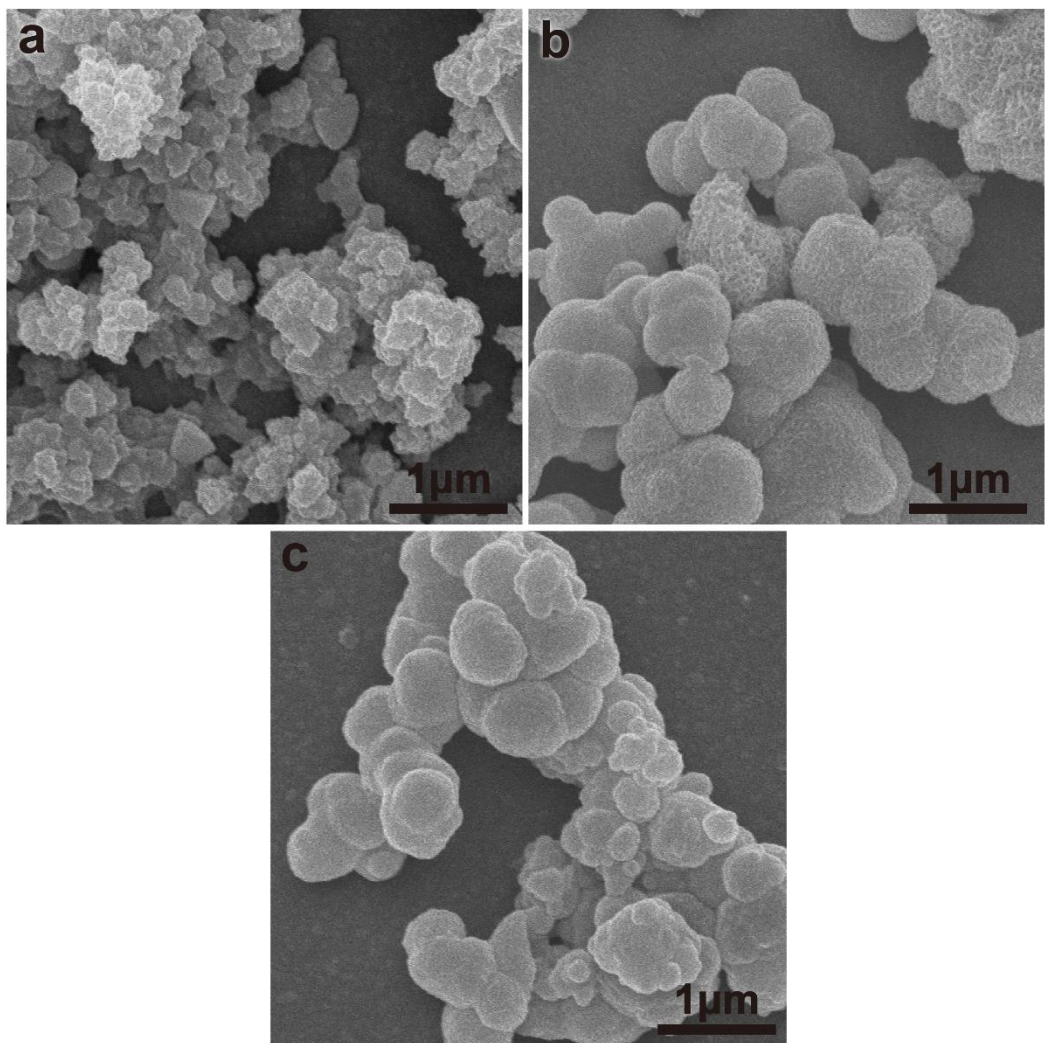


**Figure S3.** SEM images of the NiFe-LDH precursors prepared by using different amounts of urea: Instead of 11 mmol of urea, (a) 5.5 mmol, (b) 22 mmol, and (c) 33 mmol of urea was used, respectively, in the synthesis (see Experimental Section 2.2 of the main text for further details).

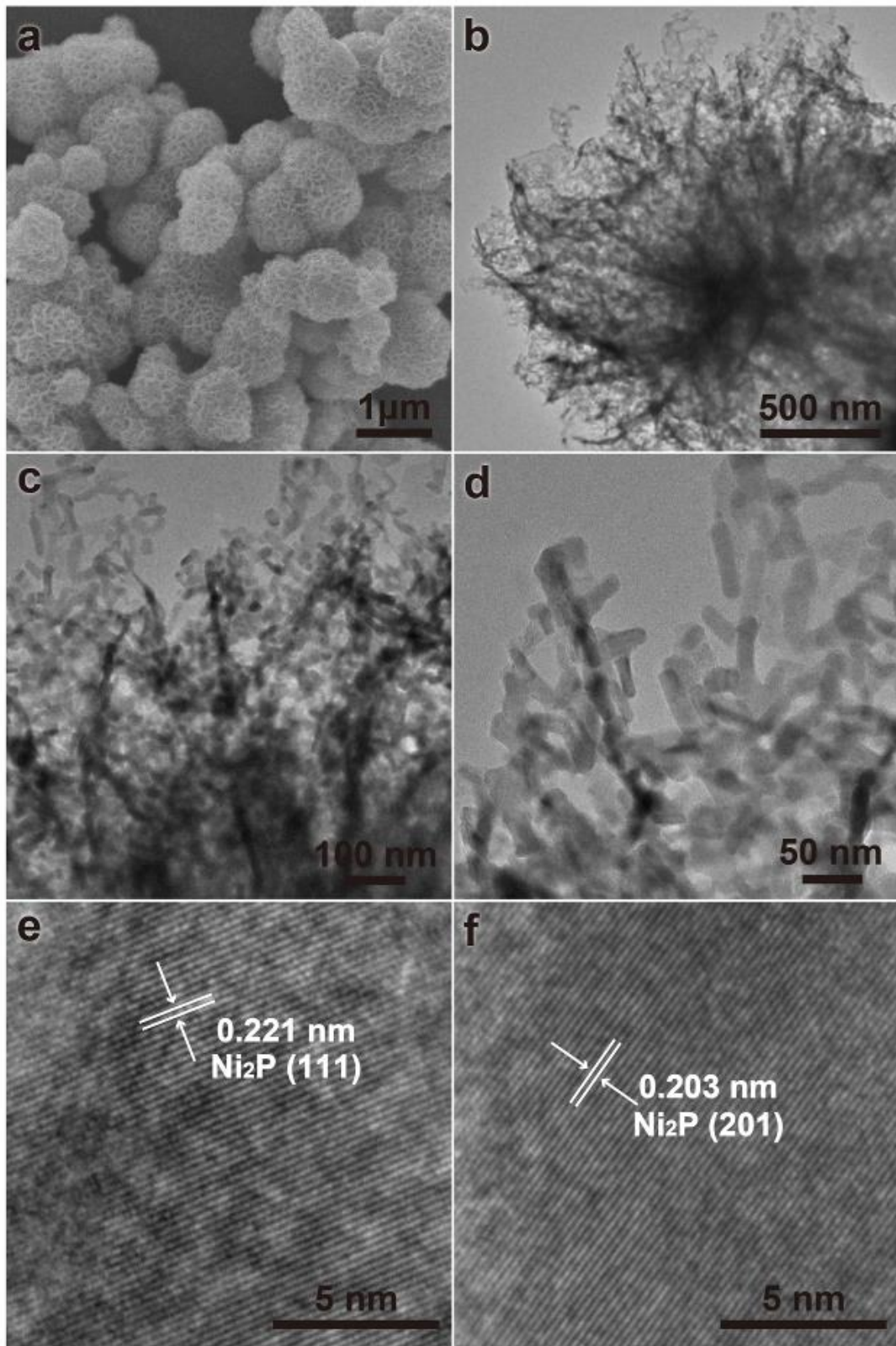


**Figure S4.** (a) SEM, (b-d) TEM, and (e, f) HRTEM images of the flowerlike NiFe(3:1)-P.

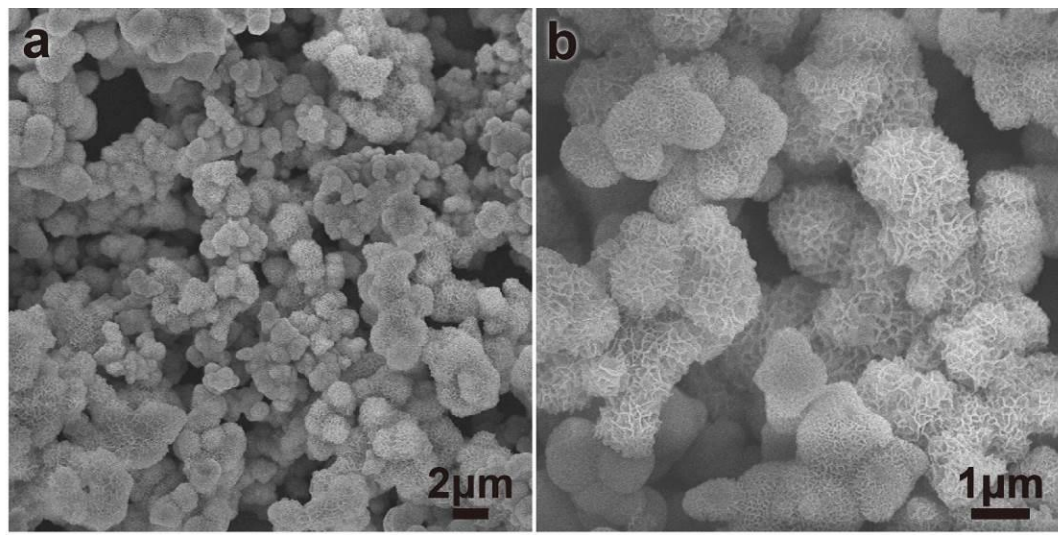


**Figure S5.** (a, b) SEM images of the flowerlike NiFe(3:1)-LDO.

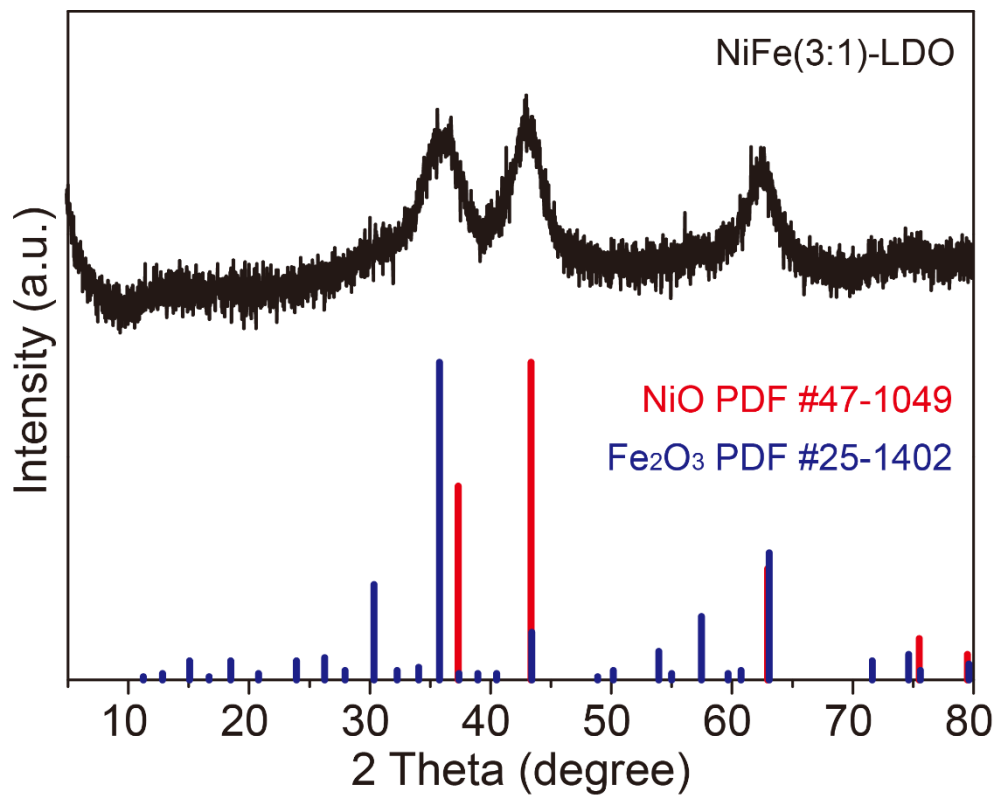


**Figure S6.** The XRD pattern of the flowerlike NiFe(3:1)-LDO.

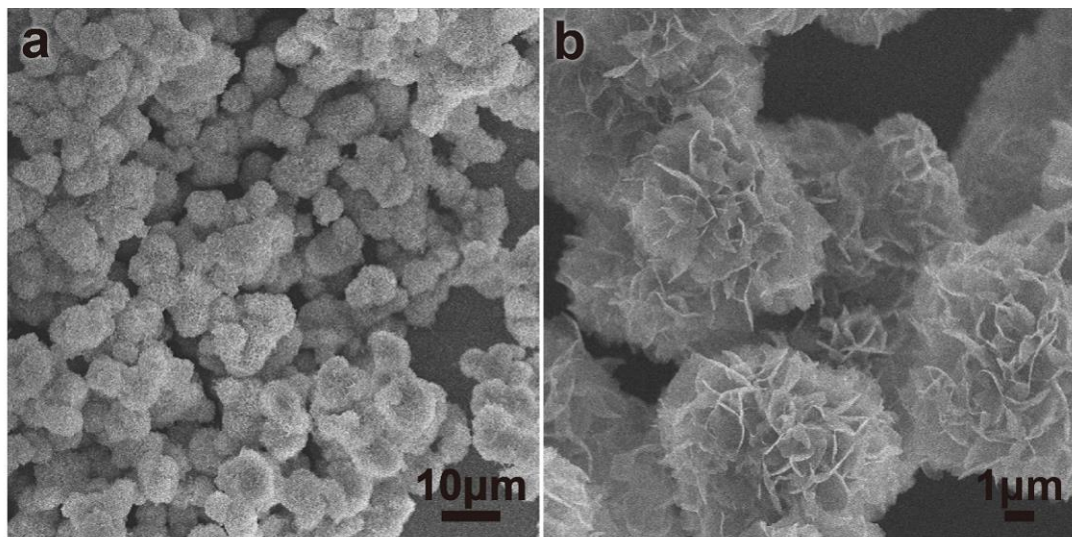


**Figure S7.** (a, b) SEM images of the flowerlike Ni-precursor.

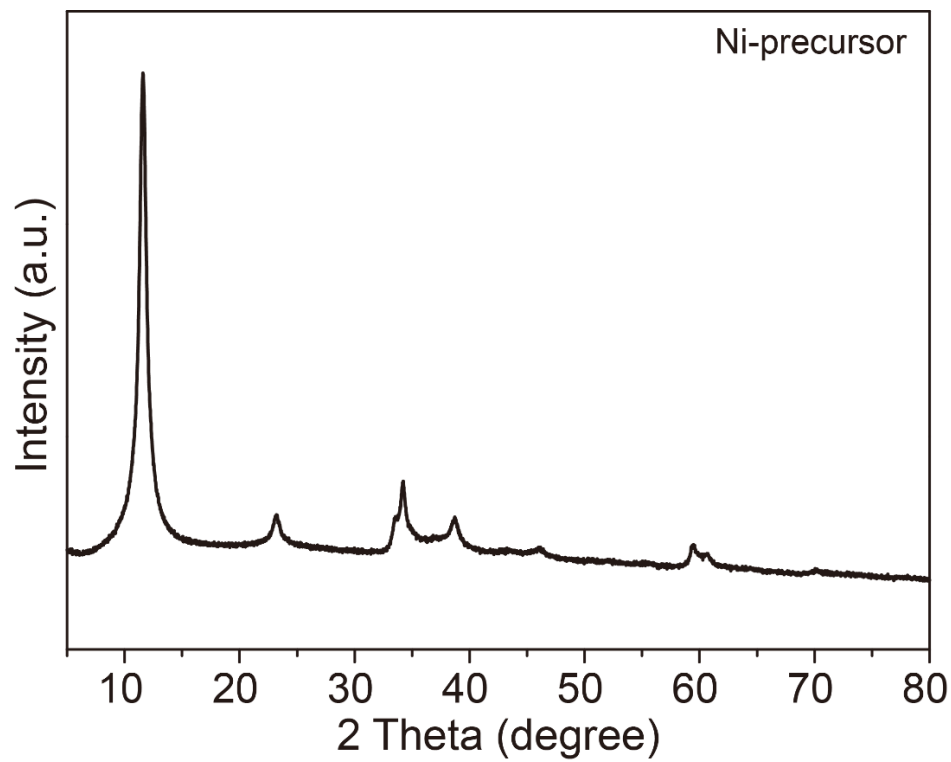


**Figure S8.** The XRD pattern of the flowerlike Ni-precursor.

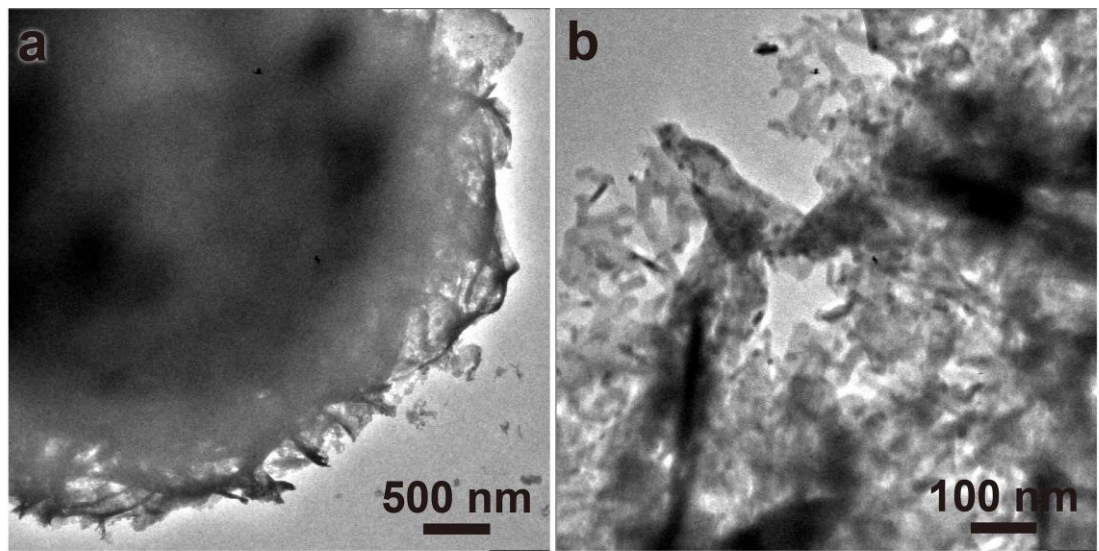


**Figure S9.** (a, b) TEM images of the flowerlike  $\text{NiP}_x$ .

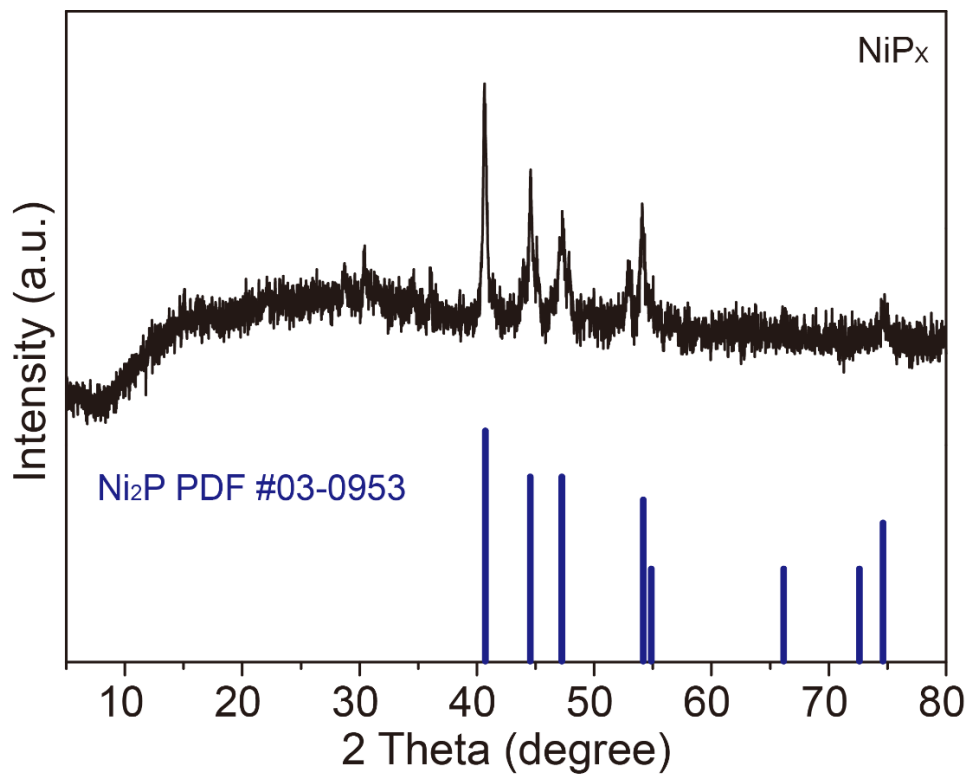


**Figure S10.** The XRD pattern of the flowerlike  $\text{NiP}_x$ .

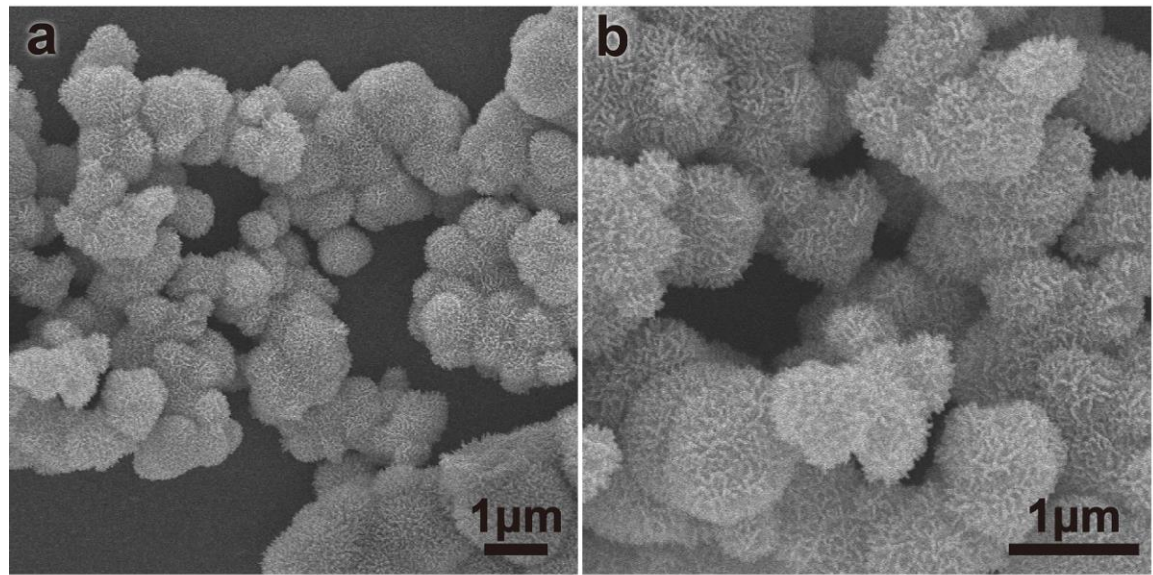


**Figure S11.** (a, b) SEM images of the flowerlike Fe-precursor.

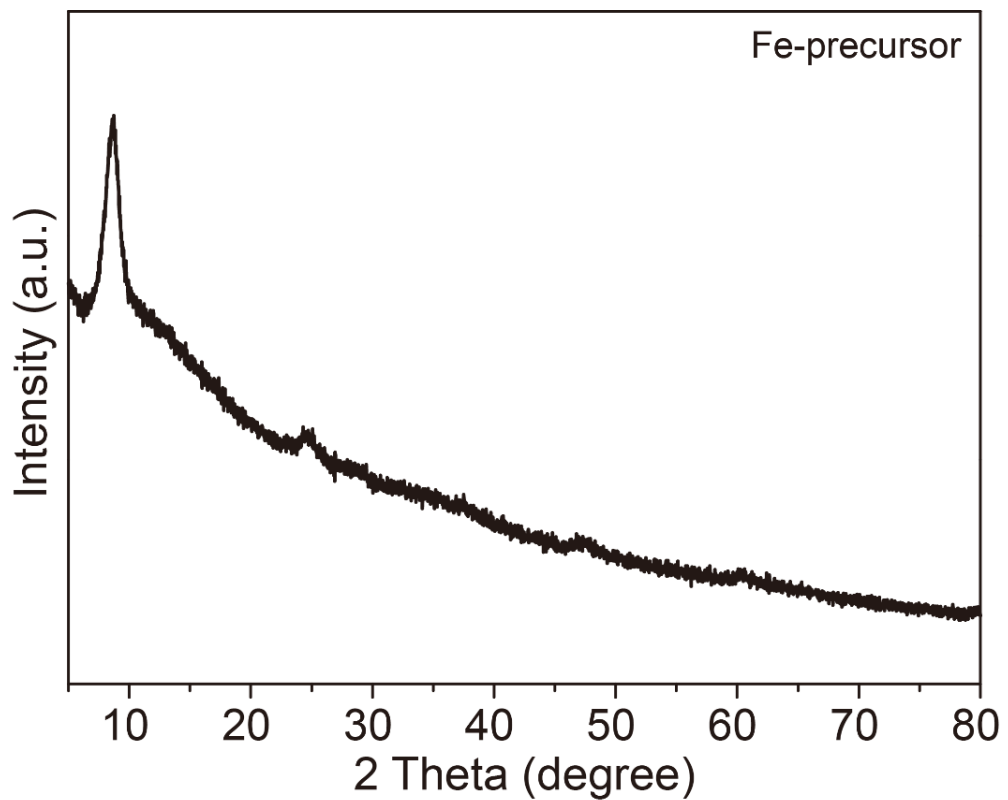


**Figure S12.** The XRD pattern of the flowerlike Fe-precursor.

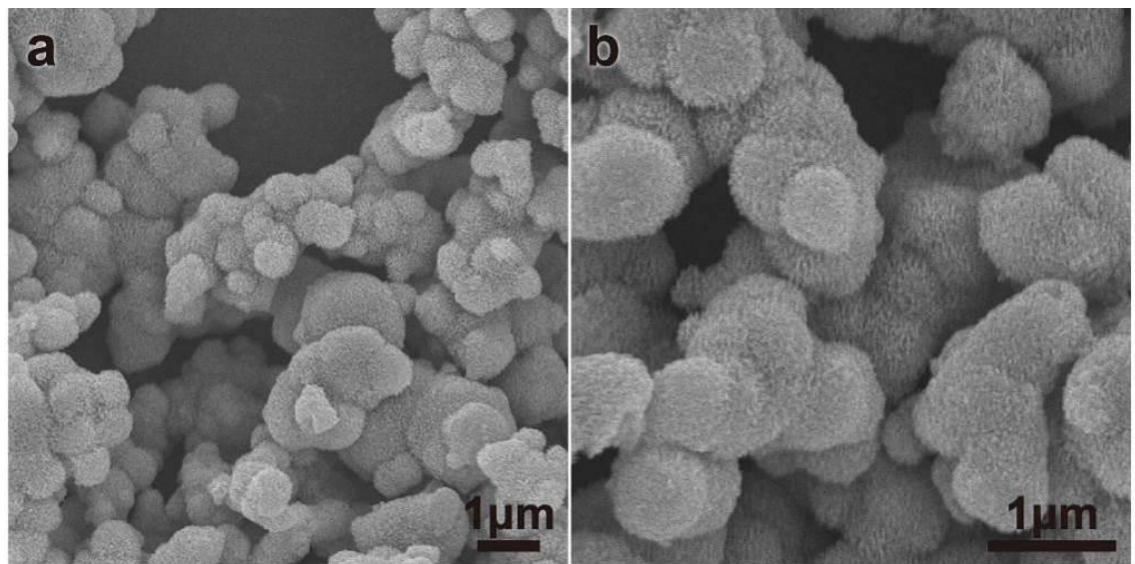


**Figure S13.** (a, b) SEM images of the flowerlike  $\text{FeP}_x$ .

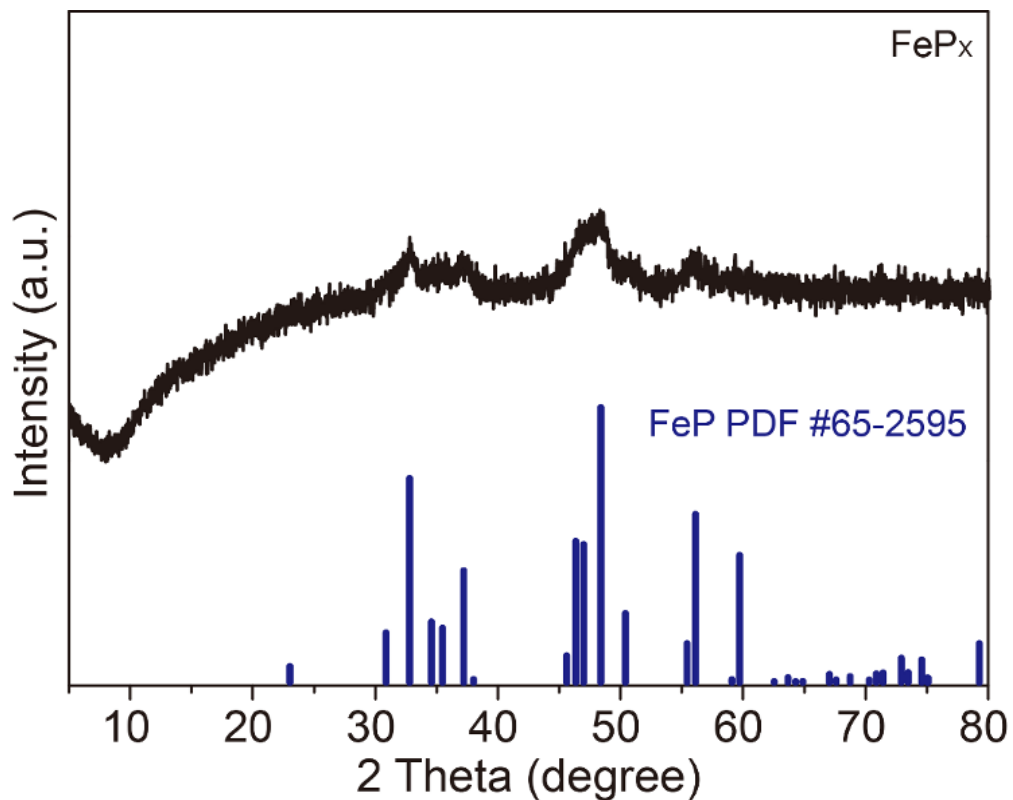


**Figure S14.** The XRD pattern of the flowerlike  $\text{FeP}_x$ .

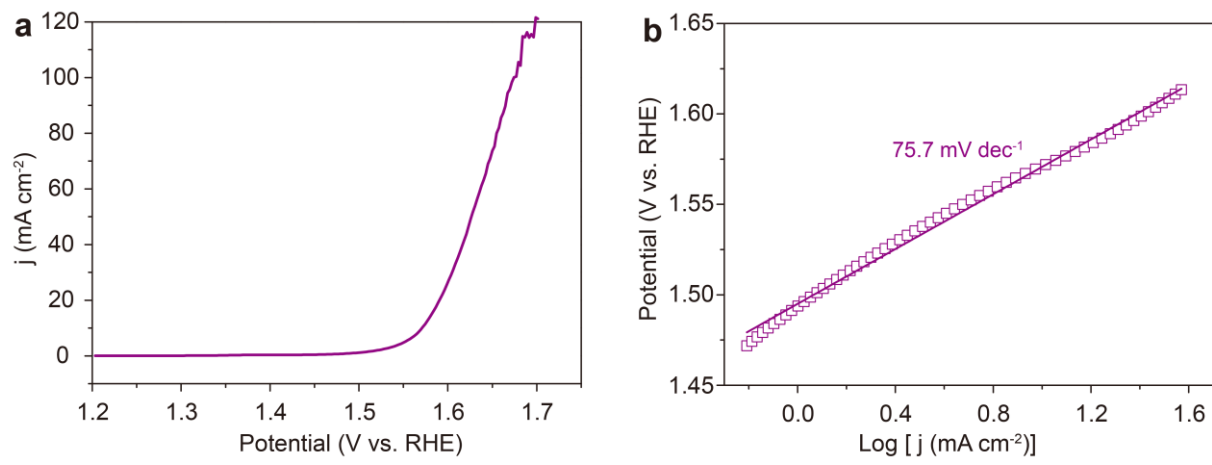


**Figure S15.** (a) The polarization curve and (b) the Tafel plot of the commercial RuO<sub>2</sub> in 1.0 M KOH.

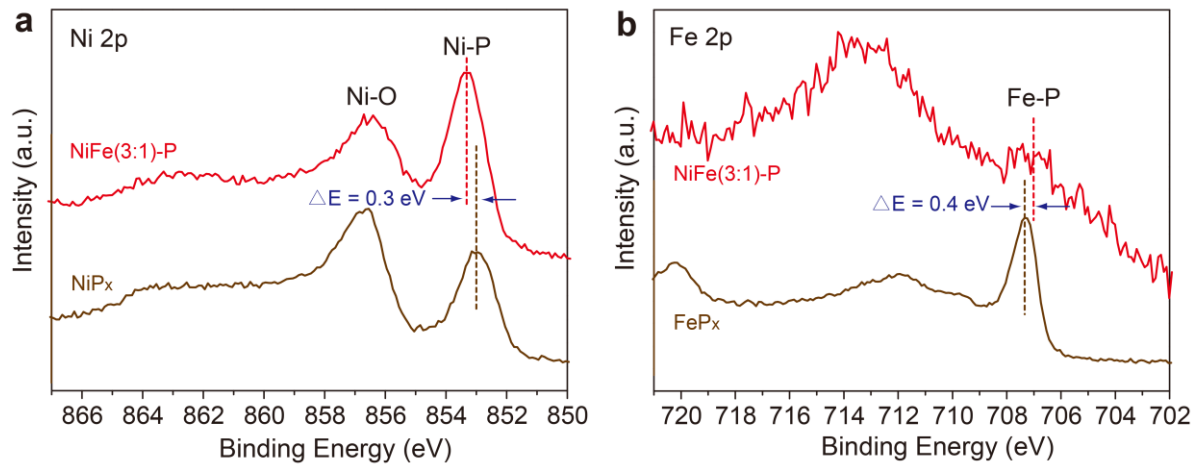


**Figure S16.** (a) Ni 2p XPS spectra of NiFe(3:1)-P and NiPx. (b) Fe 2p XPS spectra of NiFe(3:1)-P and FePx.

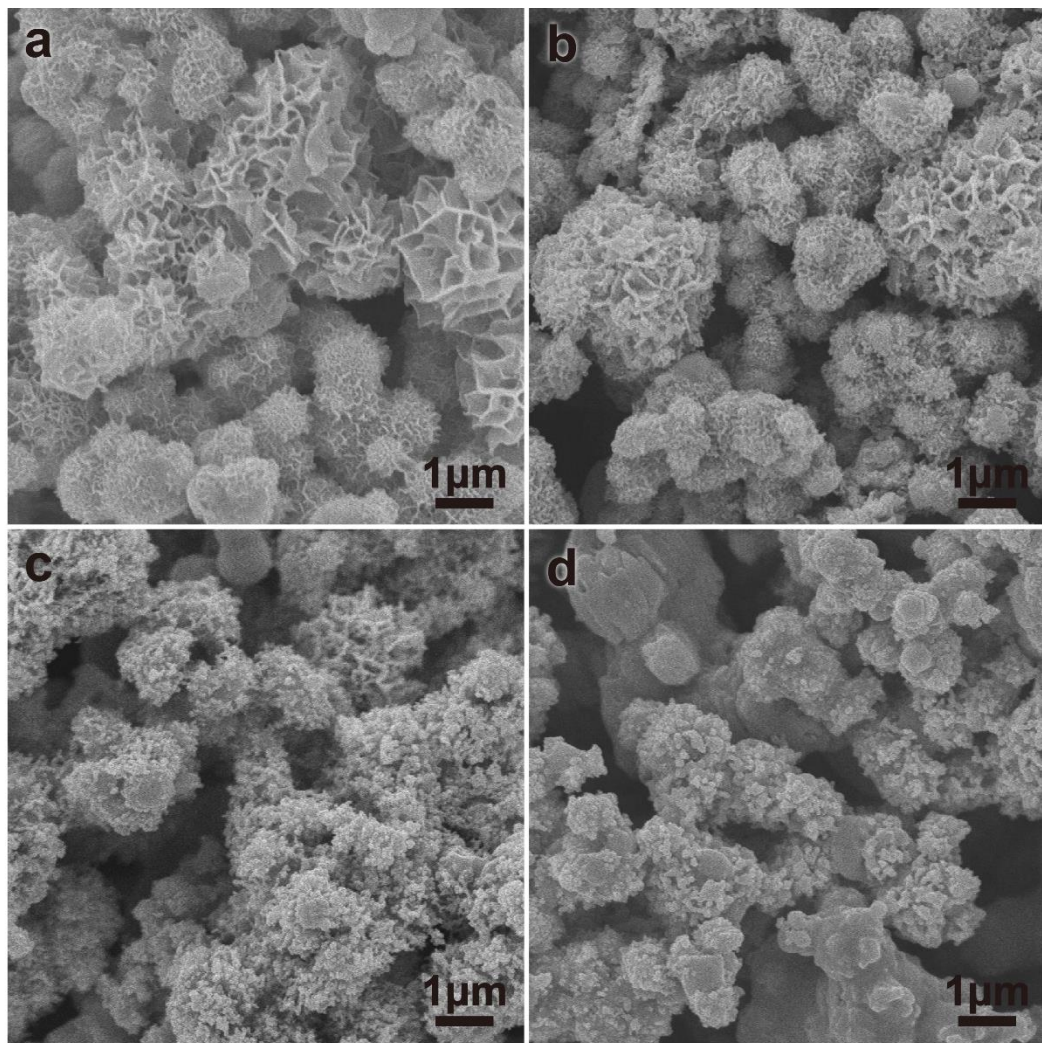


**Figure S17.** SEM images of the NiFe(3:1)-P-T obtained from different phosphidation temperatures: (a) 200 °C, (b) 400 °C, (c) 500 °C, and (d) 600 °C.

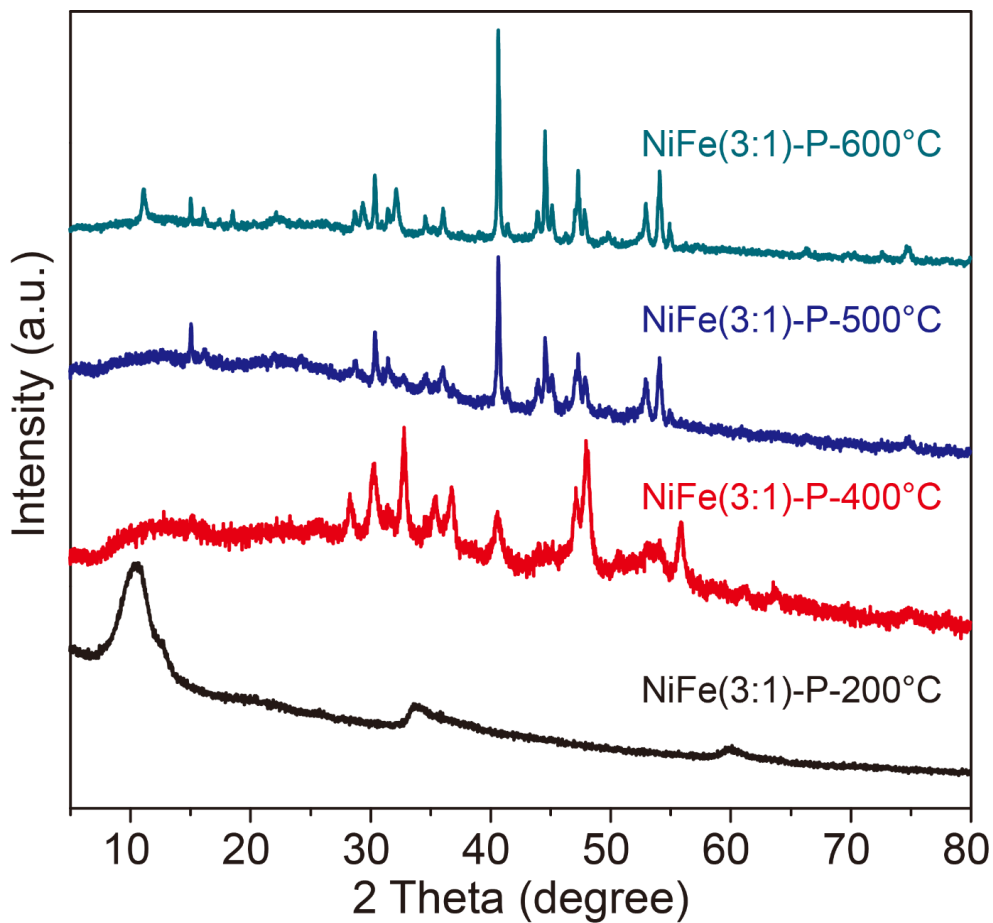


**Figure S18.** XRD patterns of the NiFe(3:1)-P-T ( $T = 200, 400, 500$ , and  $600\text{ }^{\circ}\text{C}$ ) obtained from different phosphidation temperatures.

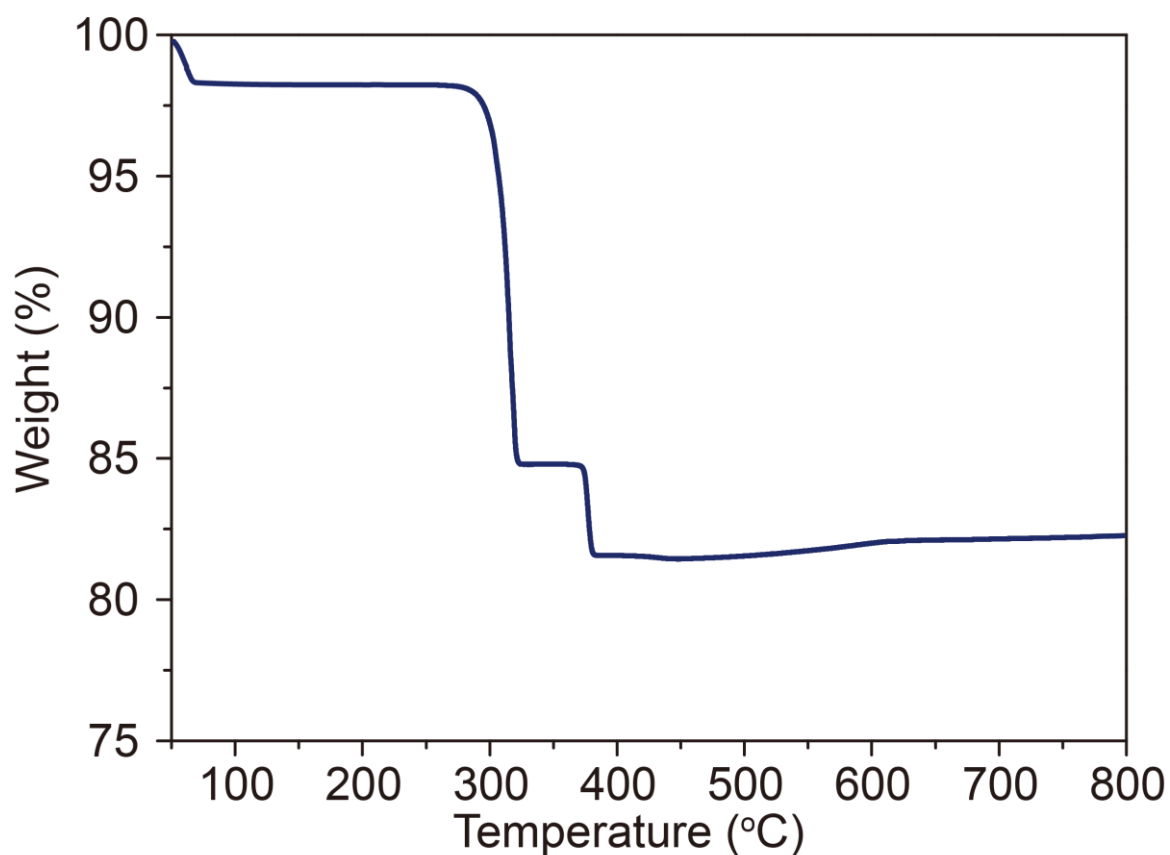


**Figure S19.** The TGA curve of  $\text{NaH}_2\text{PO}_2$ .

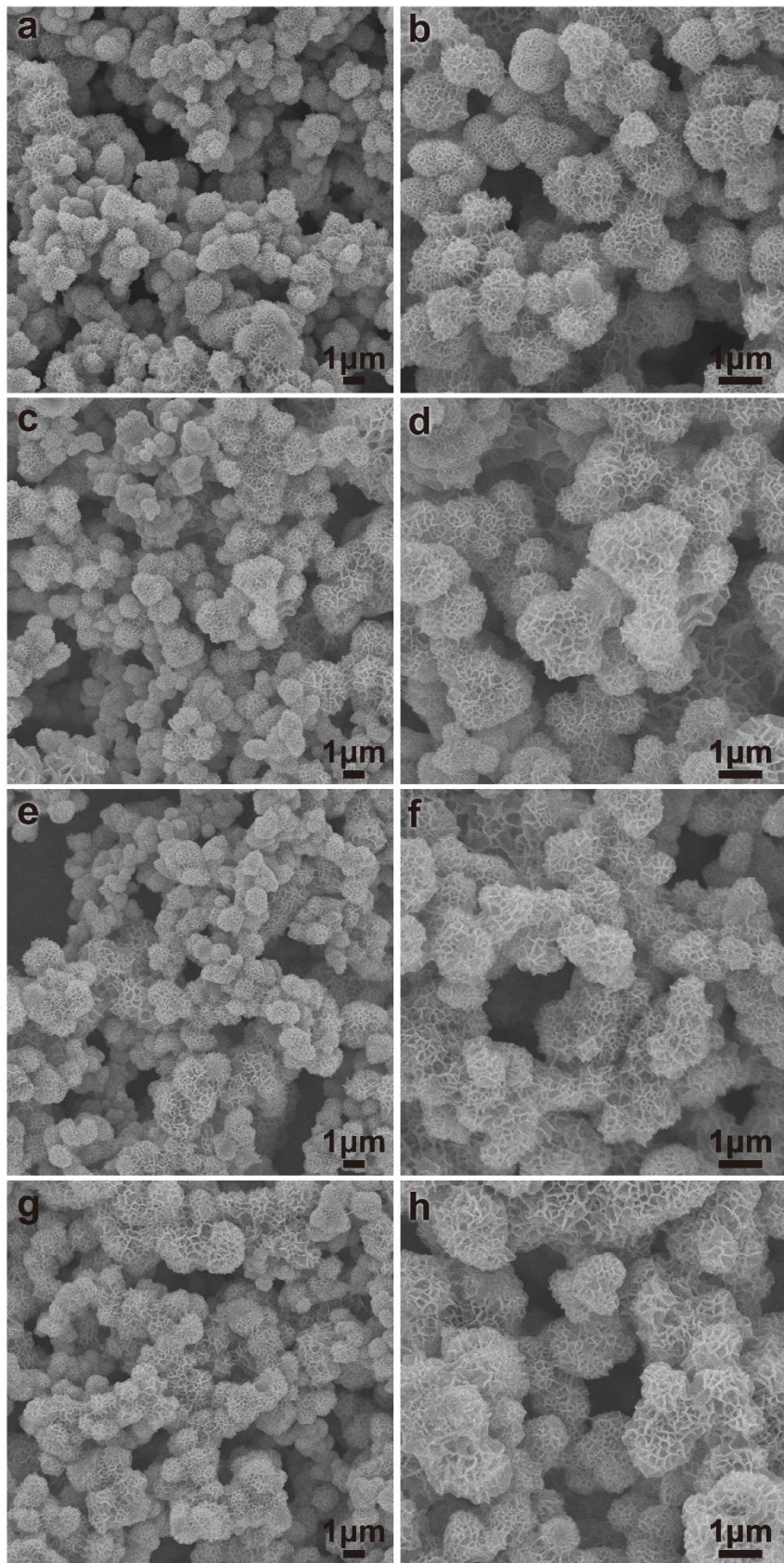


**Figure S20.** SEM images of the flowerlike NiFe(*n*:1)-LDH with different compositions: (a, b) NiFe(1:1)-LDH, (c, d) NiFe(5:1)-LDH, (e, f) NiFe(7:1)-LDH, and (g, h) NiFe(9:1)-LDH.

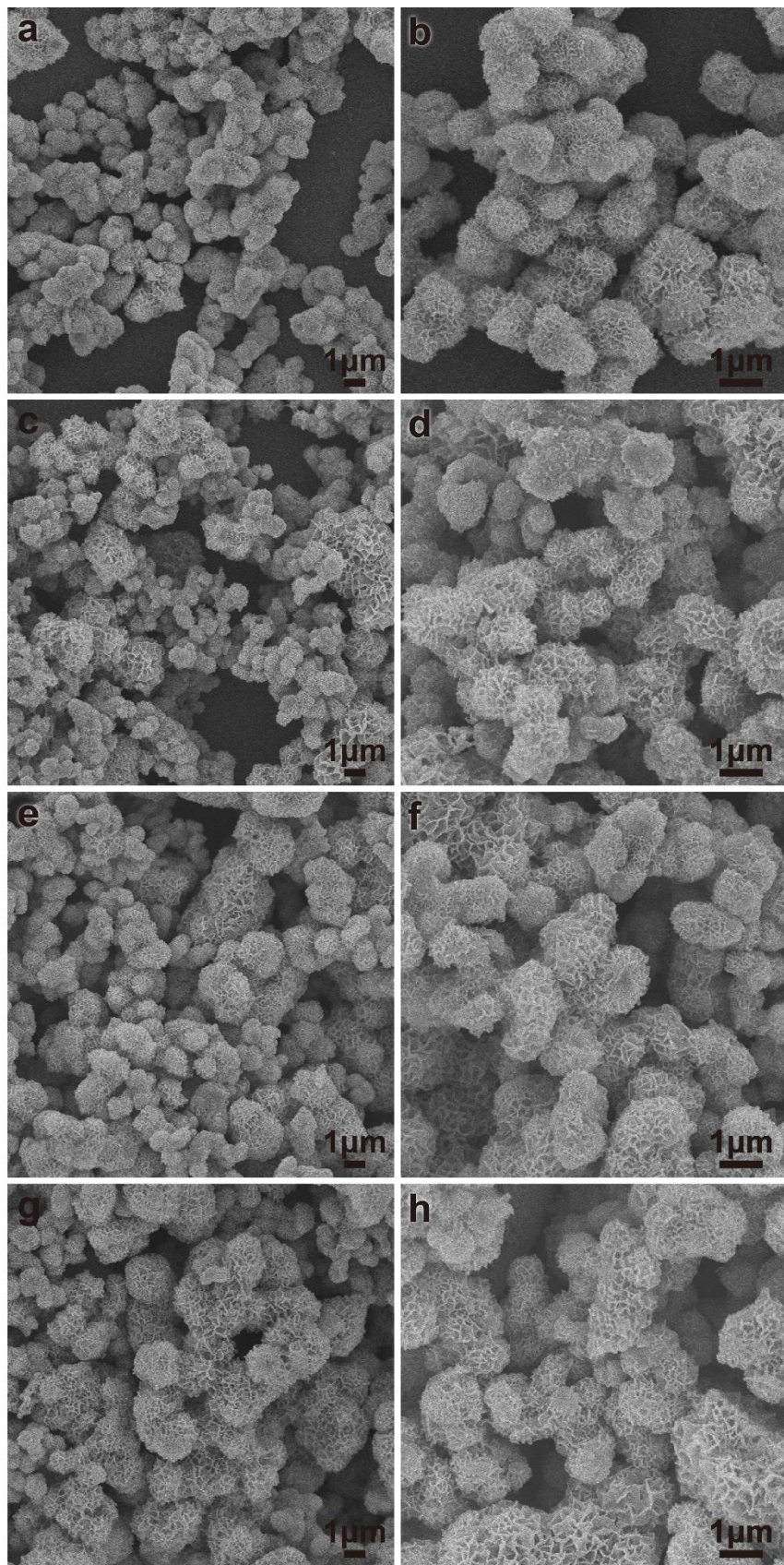


**Figure S21.** SEM images of the flowerlike NiFe( $n:1$ )-P with different compositions: (a, b) NiFe(1:1)-P, (c, d) NiFe(5:1)-P, (e, f) NiFe(7:1)-P, and (g, h) NiFe(9:1)-P.

**Table S2.** The actual molar ratios of Ni/Fe in the NiFe(*n*:1)-P samples from the ICP-OES analysis.

NiFe( <i>n</i> :1)-P	molar ratio of Ni/Fe	
	feeding ratio	actual ratio
NiFe(1:1)-P	1:1	0.80:1
NiFe(3:1)-P	3:1	2.35:1
NiFe(5:1)-P	5:1	4.17:1
NiFe(7:1)-P	7:1	6.03:1
NiFe(9:1)-P	9:1	8.12:1

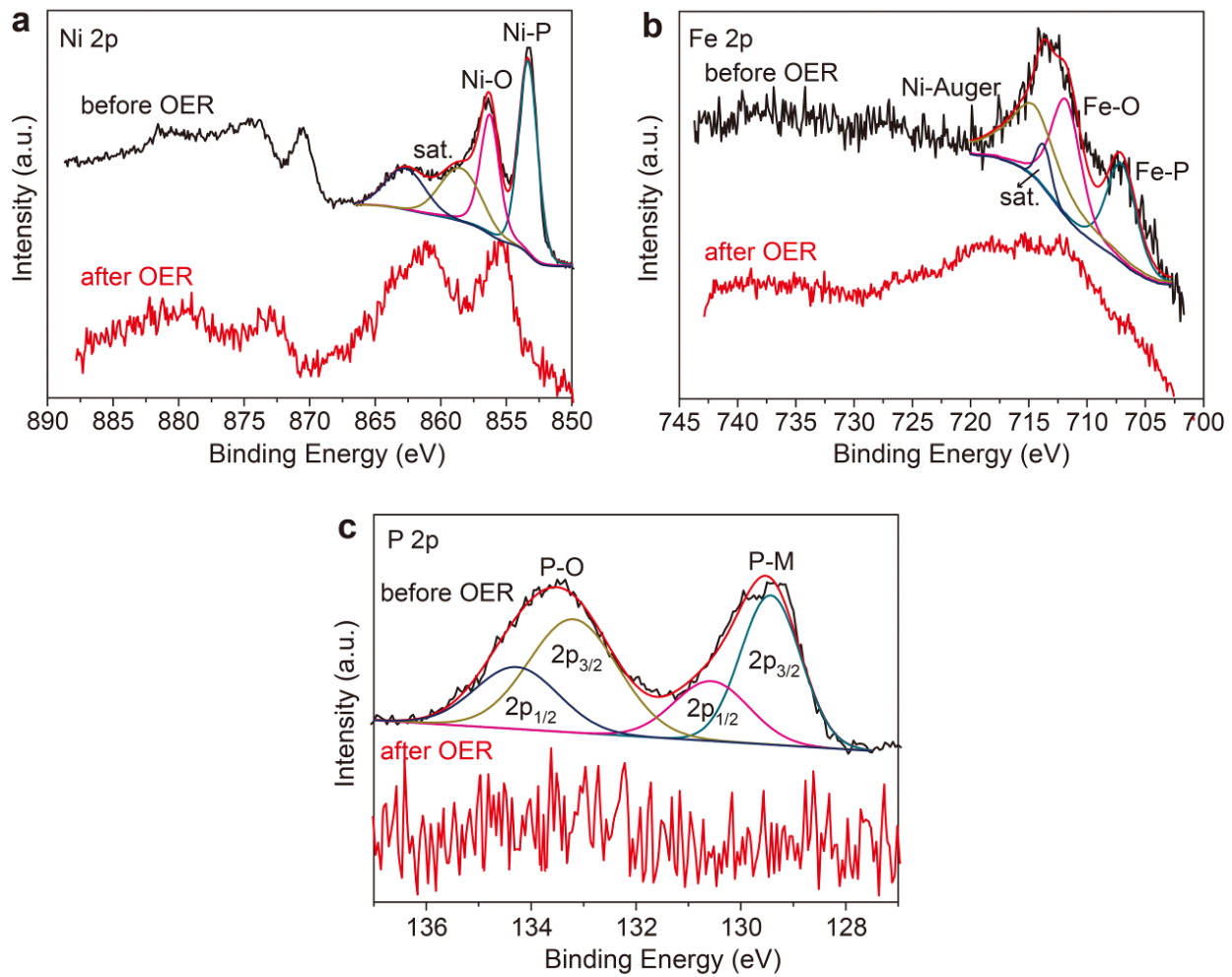


**Figure S22.** (a) Ni 2p, (b) Fe 2p, and (c) P 2p XPS spectra of the flowerlike NiFe(3:1)-P before and after OER stability test.

**Table S3.** Comparison of the OER catalytic performance of our flowerlike NiFe(3:1)-P to other recently reported high-performance OER electrocatalysts in alkaline solution.

Catalyst	Mass loading (mg cm <sup>-2</sup> )	Electrolyte	$\eta @ 10 \text{ mA cm}^{-2}$ (mV)	Tafel slope (mV dec <sup>-1</sup> )	Ref.
<b>NiFe(3:1)-P</b>	<b>0.1</b>	<b>1 M KOH</b>	<b>233</b>	<b>42.5</b>	<b>this work</b>
FeP nanorods/carbon paper	0.7	1 M KOH	350	63.6	1
FeP nanotubes	1.6	1 M KOH	288	43	2
CoP nanorods/C	0.71	1 M KOH	320	71	3
CoP/rGO	0.28	1 M KOH	340	66	4
Ni-P film	N.A.	1 M KOH	344	49	5
Ni-P nanoplates	0.2	1 M KOH	300	64	6
Ni <sub>2</sub> P nanoparticles	0.14	1 M KOH	290	59	7
Ni <sub>2</sub> P nanowires	0.14	1 M KOH	330	47	7
CoMnP NPs	0.28	1 M KOH	330	61	8
Nanoporous (Co <sub>0.52</sub> Fe <sub>0.48</sub> ) <sub>2</sub> P	N.A.	1 M KOH	270	30	9
sea-urchin-like (Co <sub>0.54</sub> Fe <sub>0.46</sub> )P <sub>2</sub>	0.2	0.1 M KOH	370	N.A.	10
NiCoP	1.6	1 M KOH	280	87	11
rGO/NiCoP	0.15	1 M KOH	270	65.7	12
NiFeP <sub>x</sub> @NPS-C	0.2	1 M KOH	265	43.0	13
Ni <sub>3</sub> N nanosheet array/carbon cloth	1.9	1 M KOH	340	N.A.	14
Fe <sub>0.1</sub> -NiS <sub>2</sub> /Ti foam	0.8	1 M KOH	191	43.0	15
Zn-Ni <sub>3</sub> S <sub>2</sub> /Ni foam	2.3	1 M KOH	N.A.	87.0	16
CoSn-hydroxide	0.66	1 M KOH	274	N.A.	17
NiFeO <sub>x</sub> film	N.A.	1 M NaOH	> 350	N.A.	18
Ni <sub>0.9</sub> Fe <sub>0.1</sub> /N-C	0.2	1 M KOH	330	45	19
Co <sub>3</sub> O <sub>4</sub> /C nanowire arrays	0.2	1 M KOH	220	61	20
Zn <sub>x</sub> Co <sub>3-x</sub> O <sub>4</sub> nanowire arrays	1.0	1 M KOH	320	51	21
Ni <sub>x</sub> Co <sub>3-x</sub> O <sub>4</sub> nanowire arrays	2.3-2.7	1 M NaOH	370	59-64	22
Amorphous NiCo <sub>2.7</sub> (OH) <sub>x</sub> nanocages	0.2	1 M KOH	350	65	23
Amorphous Ni-Co binary oxide	N.A.	1 M NaOH	325	39	24
Ni–Co mixed oxide cages	N.A.	1 M KOH	380	50	25
NiCo LDH nanosheets	0.17	1 M KOH	367	40	26

Ultrathin NiCo <sub>2</sub> O <sub>4</sub> nanosheets	0.285	1 M KOH	320	30	<sup>27</sup>
IrO <sub>x</sub>	N.A.	1 M NaOH	320 ± 40 (not stable)	N.A.	<sup>18</sup>
IrO <sub>x</sub>	N.A.	1 M KOH	427 ± 5	49 ± 1	<sup>28</sup>
IrO <sub>2</sub>	0.21	1 M KOH	338	47	<sup>29</sup>

## References:

1. D. Xiong, X. Wang, W. Li and L. Liu, *Chem. Commun.*, 2016, **52**, 8711-8714.
2. Y. Yan, B. Y. Xia, X. Ge, Z. Liu, A. Fisher and X. Wang, *Chemistry – A European Journal*, 2015, **21**, 18062-18067.
3. J. Chang, Y. Xiao, M. Xiao, J. Ge, C. Liu and W. Xing, *ACS Catal.*, 2015, **5**, 6874-6878.
4. L. Jiao, Y.-X. Zhou and H.-L. Jiang, *Chemical Science*, 2016, **7**, 1690-1695.
5. N. Jiang, B. You, M. Sheng and Y. Sun, *ChemCatChem*, 2016, **8**, 106-112.
6. X.-Y. Yu, Y. Feng, B. Guan, X. W. Lou and U. Paik, *Energy Environ. Sci.*, 2016, **9**, 1246-1250.
7. L.-A. Stern, L. Feng, F. Song and X. Hu, *Energy Environ. Sci.*, 2015, **8**, 2347-2351.
8. D. Li, H. Baydoun, C. N. Verani and S. L. Brock, *J. Am. Chem. Soc.*, 2016, **138**, 4006-4009.
9. Y. Tan, H. Wang, P. Liu, Y. Shen, C. Cheng, A. Hirata, T. Fujita, Z. Tang and M. Chen, *Energy Environ. Sci.*, 2016, **9**, 2257-2261.
10. A. Mendoza-Garcia, H. Zhu, Y. Yu, Q. Li, L. Zhou, D. Su, M. J. Kramer and S. Sun, *Angew. Chem. Int. Ed.*, 2015, **54**, 9642-9645.
11. H. Liang, A. N. Gandi, D. H. Anjum, X. Wang, U. Schwingenschlögl and H. N. Alshareef, *Nano Lett.*, 2016, **16**, 7718-7725.
12. J. Li, M. Yan, X. Zhou, Z.-Q. Huang, Z. Xia, C.-R. Chang, Y. Ma and Y. Qu, *Adv. Funct. Mater.*, 2016, **26**, 6785-6796.
13. P. Li and H. C. Zeng, *Chem. Commun.*, 2017, **53**, 6025-6028.
14. Q. Liu, L. Xie, F. Qu, Z. Liu, G. Du, A. M. Asiri and X. Sun, *Inorg. Chem. Front.*, 2017, **4**, 1120-1124.
15. N. Yang, C. Tang, K. Wang, G. Du, A. M. Asiri and X. Sun, *Nano Res.*, 2016, **9**, 3346-3354.
16. Q. Liu, L. Xie, Z. Liu, G. Du, A. M. Asiri and X. Sun, *Chem. Commun.*, 2017, **53**, 12446-12449.

17. F. Song, K. Schenk and X. Hu, *Energy Environ. Sci.*, 2016, **9**, 473-477.
18. C. C. L. McCrory, S. Jung, J. C. Peters and T. F. Jaramillo, *J. Am. Chem. Soc.*, 2013, **135**, 16977-16987.
19. X. Zhang, H. Xu, X. Li, Y. Li, T. Yang and Y. Liang, *ACS Catal.*, 2016, **6**, 580-588.
20. T. Y. Ma, S. Dai, M. Jaroniec and S. Z. Qiao, *J. Am. Chem. Soc.*, 2014, **136**, 13925-13931.
21. X. Liu, Z. Chang, L. Luo, T. Xu, X. Lei, J. Liu and X. Sun, *Chem. Mater.*, 2014, **26**, 1889-1895.
22. Y. Li, P. Hasin and Y. Wu, *Adv. Mater.*, 2010, **22**, 1926-1929.
23. J. Nai, H. Yin, T. You, L. Zheng, J. Zhang, P. Wang, Z. Jin, Y. Tian, J. Liu, Z. Tang and L. Guo, *Adv. Energy Mater.*, 2015, **5**.
24. Y. Yang, H. Fei, G. Ruan, C. Xiang and J. M. Tour, *ACS Nano*, 2014, **8**, 9518-9523.
25. L. Han, X. Y. Yu and X. W. Lou, *Adv. Mater.*, 2016, **28**, 4601-4605.
26. H. Liang, F. Meng, M. Cabán-Acevedo, L. Li, A. Forticaux, L. Xiu, Z. Wang and S. Jin, *Nano Lett.*, 2015, **15**, 1421-1427.
27. J. Bao, X. Zhang, B. Fan, J. Zhang, M. Zhou, W. Yang, X. Hu, H. Wang, B. Pan and Y. Xie, *Angew. Chem. Int. Ed.*, 2015, **54**, 7399-7404.
28. L. Trotochaud, J. K. Ranney, K. N. Williams and S. W. Boettcher, *J. Am. Chem. Soc.*, 2012, **134**, 17253-17261.
29. F. Song and X. Hu, *Nat Commun*, 2014, **5**.